Two-photon cavity solitons in purely active media

R. Vilaseca, M.C. Torrent, J. García-Ojalvo
Departament de Física i Enginyeria Nuclear, Universitat Politècnica de Catalunya, Colom 11, E-08222 Terrassa, Spain

M. Brambilla
Dipartimento di Fisica and INFM, Politecnico di Bari, Via E. Orabona 4, I-70126 Bari, Italy

M. San Miguel
Instituto Mediterráneo de Estudios Avanzados, Universitat de les Illes Balears, E-07071 Palma de Mallorca, Spain

We show that broad-area cascade lasers with no absorbing intracavity elements support the spontaneous formation of two-dimensional bright localized structures in a dark background. These cavity solitons consist of islands of two-photon emission embedded in a background of single-photon emission. We discuss the mechanisms through which these structures are formed and interact, along with their properties and stability.

PACS numbers: 42.65.Sf, 42.50.Hz, 42.65.Tg

Spatial solitons are among the most fascinating nonlinear localized structures exhibited by spatially extended systems. In an optical context, these localized structures take the form of self-trapped light beams that propagate through nonlinear media with an unperturbed transverse cross section, and result from a dynamic balance between a spreading linear mechanism (diffraction) and a nonlinear shrinking one [1]. Spatial solitons might be useful for efficient all-optical parallel signal transmission and processing.

Although spatial solitons were initially associated with conservative systems, investigations in last years have shown that similar structures can also appear in dissipative systems. Presently there is a large interest in investigating the case of a nonlinear optical medium placed within a cavity (or near a mirror), in which the influence of feedback and resonance effects leads to localized structures with distinctive qualitative and quantitative characteristics [2]. These *cavity solitons* (CS) often result from a bistability between two stationary spatially-extended states of the system, in the form of either self-trapped switching waves between two homogeneous states, or isolated pattern elements embedded in a homogeneous background. They have been predicted or observed so far in passive (i.e. externally driven) media (with absorptive/dispersive, [3–5], photorefractive [6], second-order [7], and third-order [8] nonlinearities), and also in lasers with saturable absorber [9].

Extensive studies of the spatiotemporal dynamics of two-level lasers (see e.g. [10]) seem to indicate that CSs do not exist in purely active single-photon lasers (i.e. without absorbing intracavity elements). In this paper, we show that CSs can in fact exist in purely active media, provided that single-photon amplification is complemented with *two-photon* emission processes. As we show below, the presence of these fundamental light-matter interaction phenomena (not considered in any of the cases pointed out above) leads to the formation of CSs with distinctive features, such as the spatial separation of the two types of amplification (single-photon and two-photon) that they bring about, their combined short/long interaction range, and their globally attracting character (they are the *only* stable emission regime of the system).

We consider a cascade laser, in which two fields of different frequency are simultaneously generated through their coupling with the two consecutive transitions defined by a three-level atomic system (Fig. 1). Interaction between these two fields comes through the population of the intermediate level 0 and the two-photon quantum coherence between levels 1 and 2. Transverse effects have been seen to lead in this system to coupled patterns of the two generated fields, in both low-Fresnel-number [11] and high-Fresnel-number (broad-area) [12] cavities. In what follows we will concentrate on the latter case. The spatiotemporal behavior of a cascade laser in such a situation can be described by the following Maxwell-Bloch equations [12]:

$$\begin{aligned}
\dot{\alpha}_1 &= -\sigma_1\alpha_1 + i\sigma_1\rho_{01} + ia_1\nabla^2\alpha_1 \\
\dot{\alpha}_2 &= -\sigma_2\alpha_2 + i\sigma_2\rho_{20} + ia_2\nabla^2\alpha_2 \\
\dot{\rho}_{01} &= -(1+i\delta_1)\rho_{01} - i\alpha_1 d_1 + i\sqrt{\chi}\alpha_2^*\rho_{21} + \beta_1\xi_1 \\
\dot{\rho}_{20} &= -(1+i\delta_2)\rho_{20} - i\alpha_2 d_2 - i\alpha_1^*\rho_{21}/\sqrt{\chi} + \beta_2\xi_2 \\
\dot{\rho}_{21} &= -(\Gamma+i\epsilon)\rho_{21} - i\sqrt{\chi}\alpha_1\rho_{20} + i\alpha_2\rho_{01}/\sqrt{\chi} \\
\dot{d}_1 &= -bd_1 - 2\,\mathrm{Im}(\alpha_1\rho_{01}^*) + \chi\,\mathrm{Im}(\alpha_2\rho_{20}^*) \\
\dot{d}_2 &= b(r_2-d_2) + \chi^{-1}\,\mathrm{Im}(\alpha_1\rho_{01}^*) - 2\,\mathrm{Im}(\alpha_2\rho_{20}^*)\,,
\end{aligned} \tag{1}$$

where α_1 and α_2 are the complex envelopes of the generated electric fields, ρ_{ij} the complex one- and two-photon coherences, d_1 and d_2 the population inversions of the two transitions, r_2 the pumping rate for the upper level 2, a_1 and a_2 the diffraction coefficients, σ_i, Γ and b the relaxation rates, and χ the efficiency of transition 1 versus transition 2. The cavity detunings for the two fields are given by $\delta_i \equiv \omega_{\rm tr,i} - \omega_{\rm cav,i}$ (with $\omega_{\rm tr,i}$ denoting the transition frequency and $\omega_{\rm cav,i}$ the cavity resonance frequency), and $\epsilon = \delta_1 + \delta_2$. Spontaneous emission processes are accounted for by gaussian white noise terms $\xi_i(\vec{x}, t)$ with zero mean and intensity β_i^2.

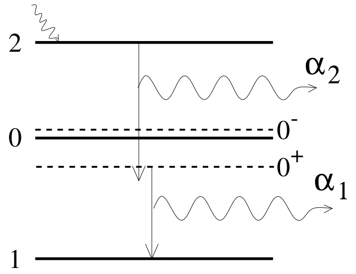

FIG. 1. Energy-level scheme of a cascade laser in two-photon resonance. Arrows indicate the cavity frequencies.

Since pumping is assumed to act only on the upper transition, laser emission occurs first, for increasing pumping rate, only in field α_2. If the cavity detuning for this field is negative ($\delta_2 < 0$), which is the situation that we will assume in what follows, then it is well known [10] that the transverse profile of the field is homogeneous and its frequency ω_L is given by the pulling formula $\delta_L = \delta_2/(\sigma_2 + 1)$, where $\delta_L = \omega_{\rm tr,2} - \omega_L$. Field α_2 induces an ac-Stark splitting of level 0 (Fig. 1), so that field α_1, when generated, has two possible resonance frequencies (Autler-Townes doublet) occurring at cavity detunings given by $\delta_1^{\pm} = \frac{1}{2}\left(-\delta_L \pm \sqrt{\delta_L^2 + 4\alpha_2^2}\right)$. These values correspond to resonance with levels 0^+ and 0^-, and are associated, for large $|\delta_2|$, to two-photon and step-by-step (i.e. single-photon) processes, respectively [13].

Let us focus on the case of two-photon resonance, $\delta_1 = \delta_1^+$. In the absence of transverse effects [$a_1 = a_2 = 0$ in Eqs. (1), homogeneous-field approximation], Fig. 2 shows (in continuous and dashed lines) the steady-state intensities versus the pump parameter r_2, for $|\delta_2|$ large ($\delta_2 = -20$) and $\delta_1 = \delta_1^+$. By increasing r_2, the zero-intensity solution first undergoes a supercritical pitchfork bifurcation (PB) at $r_2 = r_2^{\rm PB}$, leading to emission of field α_2, followed by a subcritical PB at $r_2 = r_2^{\rm th}$, which leads to emission of α_1 as well. Due to this second bifurcation, the system abruptly jumps to a two-photon branch with large intensity for both fields α_1 and α_2, because of the weak initial saturation of two-photon processes [14]. As shown in Fig. 2, two domains of bistability appear: one for $r_2^{\rm SN} < r_2 \le r_2^{\rm PB}$, involving the two-photon (upper) branch and the zero-intensity solution, and another for $r_2^{\rm PB} < r_2 \le r_2^{\rm th}$, involving the two-photon branch and the single-field branch. As will be shown below, the second of these domains will be at the origin of CS formation.

When transverse effects are taken into account, important changes take place. First, both resonances of the field α_1 with the atomic levels 0^- and 0^+ can occur simultaneously, for the same value of the cavity detuning δ_1 [13]. This is shown in Fig. 3(a), which represents the neutral stability curve (obtained from a linear stability analysis of the single-field emission regime $\alpha_1 = 0$, $\alpha_2 \neq 0$) for the same parameter values of Fig. 2. In Fig. 3(a), k represents the wavenumber of a perturbation in the form of a transverse traveling wave affecting the field α_1. Above the neutral stability curve, the perturbation grows. Minima occur at two values of $|k|$, given by $|k| = 0$ and $|k| = \sqrt{\delta_1^+/a_1}$. The first value means generation of a homogeneous field α_1 due to resonance with level 0^+ (two-photon emission). In contrast, the second value corresponds to the generation of a transverse traveling wave for α_1, which allows this field to be in resonance with level 0^- (step-by-step emission). As it also occurs in simple two-level lasers with positive detuning [10], generation of the transverse component leads to emission of a tilted wave with an increased wavenumber and frequency.

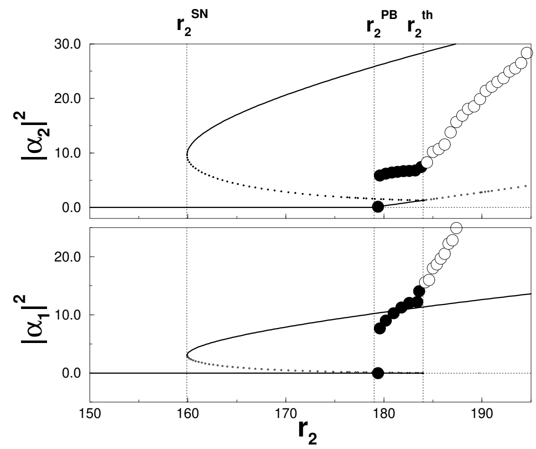

FIG. 2. Field intensity vs. pumping for a cascade laser, for $\delta_2 = -20$ and $\delta_1 = 13.33 \approx \delta_1^+$. Solid (dashed) lines: stable (unstable) steady solutions in the homogeneous-field limit. Full circles: soliton peak intensity; empty circles: time-averaged maximum peak intensity ($\sigma_1 = \sigma_2 = 0.5$, $b = \Gamma = 1$, and $\chi = 0.76$).

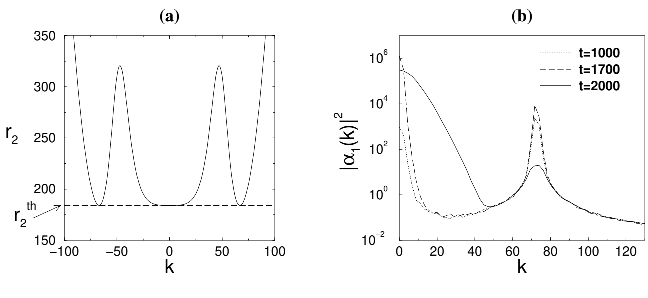

FIG. 3. (a) Neutral stability curve (field-1 emission threshold), for $\delta_2 = -20.0$ and $\delta_1 = 13.33$. (b) Spherically averaged far-field intensity profile of α_1 for $r_2 = 184$, at three different instants of time. Other parameters are those of Fig. 2, plus $a_1 = a_2 = 0.003$.

As shown in Fig. 3(a), the threshold is exactly the same for the two minima (dashed line), and coincides with that found above in the case of the homogeneous-field approximation ($r_2^{\rm th}$). Just below this threshold, the spontaneous (noise-induced) emission on field α_1 occurs predominantly through single-photon, step-by-step processes (i.e., with $|k| = \sqrt{\delta_1^+/a_1}$). However, when pumping is increased above $r_2^{\rm th}$, the smaller initial saturation of two-photon processes makes them take over the nonlinear competition between the two wavenumbers. This can be seen in Fig. 3(b), which portrays the spherically averaged far-field intensity at three instants of time, showing how the two-photon wavenumber ($|k| = 0$) eventually becomes larger (and broader) than its single-photon counterpart ($|k| = \sqrt{\delta_1^+/a_1}$). The result is that, after a short transient, emission of field α_1 occurs in the form of *cavity solitons*, as shown in Fig. 4. This figure displays typical intensity and phase profiles of the two fields [see also Figs. 5(a) and (b)]. These CS show at least three remarkable distinctive features:

(i) They appear *spontaneously* as pumping is increased above its threshold value, independently of the initial state of the system. In other words, they are the *only* stable emission state of the system: the homogeneous-field solution (Fig. 2, upper branch), as well as any other possible solution in the form of transverse travelling waves, are unstable. The CS density is a growing function of the pump power. This fact entails a response to addressing actions (e.g. via an external pulse) very different from that found in other classes of CSs: writing (erasing) a new CS leads here to the disappearance (appearance) of another CS in a nearby position. This could lead to a different class of all-optical logical operations.

(ii) The CS formation brings about a *spatial separation* between single-photon and two-photon processes, as shown by the two-photon coherence profile of Fig. 5(c): the two-photon processes accumulate in the CS, whereas all the background is formed by single-photon processes. Because of that, the soliton exhibits no population inversion between levels 0 and 1 [Fig. 5(d)], and the noisy background of field α_1 [Fig. 4(c)] exhibits the dominant transverse wavenumber corresponding to the outer minimum of Fig. 3(a). These facts may indicate that CS formation is related to the homogeneous-field bistability domain $r_2^{\rm PB} < r_2 < r_2^{\rm th}$ (Fig. 2). However, instead of a homogeneous background in field α_2 [as would correspond to the lower stable branch in Fig. 2] one finds sharp concentric outward-travelling rings surrounding the central peak, shown in Figs. 4(b,d) and 5(b), which drain energy from that peak. Surprisingly, we have found no supercritical Hopf bifurcation that might be at the origin of these rings [15].

(iii) The spatial profiles of the two fields α_1 and α_2 are very different: whereas field α_1 displays a strongly localized structure similar to that of bright solitons in many other optical systems, field α_2 extends up to relatively long distances. This fact gives rise to a combined short/long interaction range which contrasts with the properties of standard CSs (e.g., the soliton packing density is here more limited than usual), and leads to interesting dynamics: the structures are well shaped and localized in field α_1, but at the same time they can interact (through field α_2) with other relatively distant CSs. For instance, in Figs. 4(b,d) the interaction (through periodic boundary conditions) with CSs existing in nearby cells is noticeable through ring's interferences. At low pumping rates, this interaction is small and controllable, and might be potentially useful for applications.

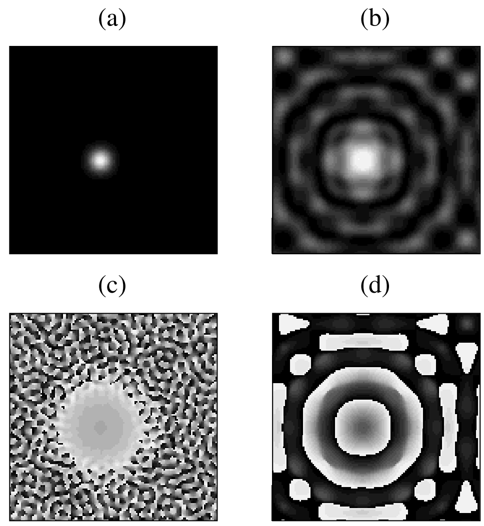

FIG. 4. Transverse emission of a broad-area cascade laser for the parameters of Fig. 3(a), plus $r_2 = 185$ and $\beta_1 = \beta_2 = 10^{-5}$: intensity (a,b) and phase (c,d) profiles of fields α_1 (a,c) and α_2 (b,d). In all plots, maxima is represented by white, and minima by black. In the phase plots, the scale ranges from $-\pi$ to $+\pi$.

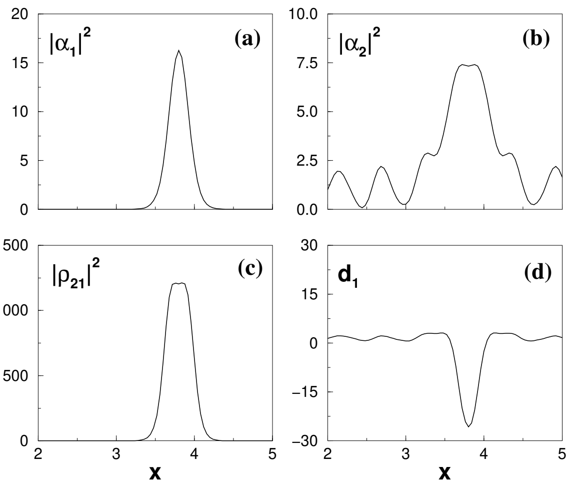

FIG. 5. Radial 1-d section of a 2-d cavity soliton, for the parameters of Fig. 3(a), plus $r_2 = 184$ and $\beta_1 = \beta_2 = 10^{-6}$.

For increasing pumping, as the CS density increases, the interaction mentioned above leads to complex dynamics, eventually producing turbulent motion and birth/death of solitons. Empty circles in Fig. 2 correspond to this regime (full circles denote stable CS), and represent a time-averaged maximum intensity of the field. A snapshot of this situation is shown in Fig. 6. It should be noted that, in spite of the interaction, each CS has its own (time-varying) phase, not shared with other CSs due to the absence of a coupling background, and to the turbulent evolution of each individual soliton. This contrasts with CSs found in passive cavities [4]. Details of this regime will be given elsewhere.

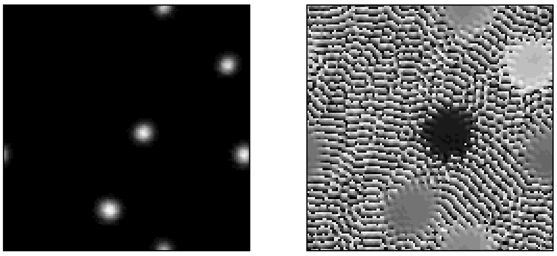

FIG. 6. Interacting cavity solitons: intensity (left) and phase (right) profiles of α_1 for the parameters of Fig. 3(a), plus $r_2 = 190$ and $\beta_1 = \beta_2 = 10^{-6}$.

For even larger pump rates ($r_2 \gtrsim 190$ in this case), CSs widen and start to loose their circular shape. For $r_2 \gtrsim 200$, most of the transverse plane becomes illuminated and the dynamics is dominated by optical vortices. A similar route from CS- to vortex-dominated dynamics has been described in [16]. Finally, we have checked that the CS state described here persists up to very large values of the cavity detuning δ_2 (up to $\delta_2 \sim -50$, at least), provided δ_1 remains relatively close to δ_1^+ (for other values of δ_1, only uniform travelling-wave solutions are found [17]).

In conclusion, we have shown that cavity solitons can appear spontaneously in purely active optical media, as a result of the interplay between two-photon and single-photon processes. They show some singular features that have not (or have only partially) been met in other optical systems investigated so far. The recent experimental realization of two-photon amplification [18] sheds hope on the possibility of observing this phenomenology.

We acknowledge financial support from DGESIC (Spain) and Generalitat de Catalunya.

[1] G.I. Stegeman and M. Segev, Science **286**, 1518 (1999).
[2] L.A. Lugiato, M. Brambilla and A. Gatti, Adv. in At., Mol. and Opt. Phys. **40**, 229 (1999); W. Firth and G. Harkness, Asian J. Phys. **7**, 665 (1998).
[3] N.N. Rosanov and G.V. Khodova, J. Opt. Soc. Am. B **7**, 1065 (1990); M. Tlidi, P. Mandel, and R. Lefever, Phys. Rev. Lett. **73**, 640 (1994); M. Kreuzer, H. Gottschling, T. Tschudi, and R. Neubecker, Mol. Cryst. Liq. Cryst. **207**, 219 (1991); W.J. Firth and A.J. Scroggie, Phys. Rev. Lett. **76**, 1623 (1996); M. Brambilla, L.A. Lugiato, and M. Stefani, Europhys. Lett. **34**, 109 (1996).
[4] M. Brambilla, L.A. Lugiato, F. Prati, L. Spinelli, and W.J. Firth, Phys. Rev. Lett. **79**, 2042 (1997); D. Michaelis, U. Peschel, and F. Lederer, Phys. Rev. A **56**, R3366 (1997).
[5] A. Schreiber, B. Thuring, M. Kreuzer, and T. Tschudi, Opt. Commun. **136**, 415 (1997); B. Schäpers, M. Feldmann, T. Ackemann, and W. Lange, Phys. Rev. Lett. **85**, 748 (2000); R. Gallego, M. San Miguel, and R. Toral, Phys. Rev. E **61**, 2241 (2000); V.J. Sánchez-Morcillo, I. Pérez-Arjona, F. Silva, G.J. de Valcárcel, and E. Roldán, Opt. Lett. **25**, 957 (2000).
[6] M. Saffman, D. Montgomery, and D.Z. Anderson, Opt. Lett. **19**, 518 (1994).
[7] V.J. Sánchez-Morcillo, E. Roldán, G.J. de Valcárcel, and K. Staliunas, Phys. Rev. A **56**, 3237 (1997); S. Longhi, Phys. Scripta **56**, 611 (1997); G.L. Oppo, A.J. Scroggie, and W.J. Firth, J. Opt. B **1**, 133 (1999); M. Le Berre, D. Leduc, E. Ressayre, and A. Tallet, J. Opt. B **1**, 153 (1999); C. Etrich, U. Peschel, and F. Lederer, Phys. Rev. Lett. **79**, 2454 (1997).
[8] V.B. Taranenko, K. Staliunas, and C.O. Weiss, Phys. Rev. Lett. **81**, 2236 (1998).
[9] V.Y. Bazhenov, V.B. Taranenko, and M.V. Vasnetsov, Proc. SPIE **1840**, 183 (1992); N.N. Rosanov, S.V. Fedorov, and G.V. Khodova, Physica D **96**, 272 (1996); V.B. Taranenko, K. Staliunas, and C.O. Weiss, Phys. Rev. A **56**, 1582 (1997).
[10] P.K. Jakobsen, J.V. Moloney, A.C. Newell, and R. Indik, Phys. Rev. A **45**, 8129 (1992).
[11] J. García-Ojalvo, M.C. Torrent, R. Vilaseca, and M. Brambilla, Chaos, Solitons & Fractals **10**, 819 (1999).
[12] J. García-Ojalvo, R. Vilaseca, and M.C. Torrent, Phys. Rev. A **56**, 5111 (1997).
[13] J. García-Ojalvo, R. Vilaseca, and M.C. Torrent, Europhys. Lett. **43**, 261 (1998).
[14] E. Roldán, G.J. de Valcárcel, R. Vilaseca, and V. Espinosa, J. Mod. Opt. **44**, 83 (1997).
[15] M. Tlidi and P. Mandel, Phys. Rev. A **59**, 2575 (1999).
[16] C.O. Weiss, M. Vaupel, K. Staliunas, G. Slekys, and V.B. Taranenko, Appl. Phys. B **68**, 151 (1999).
[17] M.C. Torrent, R. Vilaseca, and J. García-Ojalvo, J. Opt. B **2**, 432 (2000).
[18] O. Pfister, W.J. Brown, M.D. Stenner, and D.J. Gauthier, Phys. Rev. A **60**, R4249 (1999).